

Article

In Vivo Incorporation of Photoproteins into GroEL Chaperonin Retaining Major Structural and Functional Properties

Victor Marchenkov ¹, Tanya Ivashina ², Natalia Marchenko ¹ , Natalya Ryabova ¹, Olga Selivanova ¹, Alexander Timchenko ¹, Hiroshi Kihara ³, Vladimir Ksenzenko ¹ and Gennady Semisotnov ^{1,*} 

¹ Institute of Protein Research, Russian Academy of Sciences, 4 Institutskaya St., 142290 Pushchino, Russia

² Skryabin Institute of Biochemistry and Physiology of Microorganisms, Russian Academy of Sciences, 5 Prospect Nauki, 142290 Pushchino, Russia

³ Department of Physics, Kansai Medical University, Shin-Machi 2-5-1, Hirakata 573-1010, Japan

* Correspondence: nina@vega.protres.ru; Tel.: +7-(496)-731-8409

Abstract: The incorporation of photoproteins into proteins of interest allows the study of either their localization or intermolecular interactions in the cell. Here we demonstrate the possibility of in vivo incorporating the photoprotein *Aequorea victoria* enhanced green fluorescent protein (EGFP) or *Gaussia princeps* luciferase (GLuc) into the tetradecameric quaternary structure of GroEL chaperonin and describe some physicochemical properties of the labeled chaperonin. Using size-exclusion and affinity chromatography, electrophoresis, fluorescent and electron transmission microscopy (ETM), small-angle X-ray scattering (SAXS), and bioluminescence resonance energy transfer (BRET), we show the following: (i) The GroEL₁₄-EGFP is evenly distributed within normally divided *E. coli* cells, while gigantic undivided cells are characterized by the uneven distribution of the labeled GroEL₁₄ which is mainly localized close to the cellular periplasm; (ii) EGFP and likely GLuc are located within the inner cavity of one of the two GroEL chaperonin rings and do not essentially influence the protein oligomeric structure; (iii) GroEL₁₄ containing either EGFP or GLuc is capable of interacting with non-native proteins and the cochaperonin GroES.

Keywords: GroEL chaperonin; photoproteins; protein–protein interactions; protein oligomerization; cell division



Citation: Marchenkov, V.; Ivashina, T.; Marchenko, N.; Ryabova, N.; Selivanova, O.; Timchenko, A.; Kihara, H.; Ksenzenko, V.; Semisotnov, G. In Vivo Incorporation of Photoproteins into GroEL Chaperonin Retaining Major Structural and Functional Properties. *Molecules* **2023**, *28*, 1901. <https://doi.org/10.3390/molecules28041901>

Academic Editor: Luca Federici

Received: 10 January 2023

Revised: 12 February 2023

Accepted: 14 February 2023

Published: 16 February 2023



Copyright: © 2023 by the authors. Licensee MDPI, Basel, Switzerland. This article is an open access article distributed under the terms and conditions of the Creative Commons Attribution (CC BY) license (<https://creativecommons.org/licenses/by/4.0/>).

1. Introduction

Chaperonins are oligomeric ring-shaped proteins forming seven- to nine-fold symmetric one- or double-ring complexes of 500–1000 kDa, resulting in one or two extensive inner cavities [1–3]. They are widely distributed in various organisms and play an essential role in the proteostasis network, including the facilitation of protein folding and transport and the prevention of protein misfolding and aggregation [1,4–7]. Despite the relatively low sequence identity between chaperonins from different organisms, their spatial structures are very similar [2,8,9]. Each subunit of a chaperonin consists of three domains: apical, intermediate, and equatorial [8–10], whose allosteric conformational changes are induced by Mg-ATP binding, while its hydrolysis is crucial for chaperonin functioning [11–14].

On the top of apical domains, there are hydrophobic clusters responsible for binding to various hydrophobic species of both high (denatured or non-native proteins) and low molecular weight (various peptides and drugs [8,15–18]). Equatorial domains contain adenylyl nucleotide binding sites and provide the majority of interactions both between the subunits and between the rings [8,13,14]. The protein C- and N-ends are located close to each other within equatorial domains in the protein's inner cavity [8]. The intermediate domains act as hinges between apical and equatorial domains, providing allosteric conformational changes [8,13,19]. The functional and structural peculiarities of chaperonins are of importance due to their potential usage in biotechnology and biomedicine projects [18,20–23]. Some investigators used fusions within the GroEL cavity to produce

toxic or prone-to-aggregation polypeptides [21,22], while others employed the tight binding of hydrophobic drugs by GroEL apical domains for the delivery of these drugs to tumors [18]. Works on the direct incorporation of polypeptides into GroEL-like chaperonins are not numerous. For example, in the work of Kyratsous et al. [24], two proteins, which are normally insoluble during bacterial expression, mouse prion protein PrP and Varicella Zoster virus protein ORF21p, were used as a fusion part of the GroEL subunit. The authors used a vector where the sequence of a target polypeptide is placed in frame at the carboxy terminus of the GroEL subunit and demonstrated that these fusion constructs are expressed in large amounts in a soluble form [24]. Similarly, usually insoluble *Shigella's* IpaB antigen domain was fused with GroEL from *Salmonella enterica* Typhi bacteria to receive a fusion product for the immunization of mice [25]. Unfortunately, no analysis of the location of fused target proteins within GroEL oligomeric structure was made in these works, and the authors explained the effect of increased solubility by an increase in the chaperonin local concentration near the folding target protein. However, a set of bacterial expression vectors has been published that allows fusing the target protein with GroEL for its subsequent expression in a soluble, easily purified form [26]. A more thoughtful strategy was used by Fedorov's group to introduce in GroEL some toxic-to-cell and prone-to-aggregation polypeptides. The peptide was inserted into the GroEL polypeptide chain in such a way that it did not interfere with the formation of the correct GroEL oligomeric structure, but protruded into the oligomer cavity and interacted with the substrate-binding surface. For this purpose, a methionineless variant of thermostable chaperon GroEL from *Thermus thermophilus* was designed [27], and two target peptides—a toxic antimicrobial polypeptide polyphemusin I [22] and a therapeutic peptide for the treatment of AIDS patients enfuvirtide [28]—were used. In both cases, the polypeptide fused with GroEL was expressed with high yield in a soluble state, and the target polypeptide was separated from GroEL by CNBr cleavage. It should be noted that in the case of enfuvirtide, the fusion protein was expressed as a monomer and not as an oligomer. The authors attribute this to the effect of electrostatic repulsion [22,23]. Another interesting approach was used to incorporate a target protein into the oligomeric double-ring structure of *Thermococcus* sp. KS-1 chaperonin α -subunit (TCP) [21]. Expression plasmids carried four TCP genes ligated head to tail in phase and a target protein gene at the 3' end of the linked TCP genes. As a reporter test, protein GFP was used. The final fusion protein was double-ring oligomeric, possessed green fluorescence, and electron microscopy image analyses indicated that the GFP was accommodated in the central cavity. Using this strategy, TCP fusions with two virus proteins toxic to host cells or two antibody fragments prone to aggregation were well expressed as double-ring complexes in the soluble fraction of *E. coli* [21].

Still, the incorporation of a protein of interest into the chaperonin inner cavity is tricky and requires a special approach. It depends on the protein size and the volume of the chaperonin inner cavity [21]. Moreover, a bulky protein fused with the chaperonin subunit hampers the formation of the chaperonin native oligomeric structure. To overcome this difficulty, a special design and technology of protein incorporation into the chaperonin cavity have been developed [21]. Here we propose a simple method of incorporation of photoproteins (and likely other proteins) of appropriate size fused with the GroEL subunit C-end into the inner cavity of tetradecameric GroEL chaperonin.

The photoproteins used in this study are the enhanced green fluorescent protein (EGFP), 27 kDa, and *Gaussia princeps* luciferase (GLuc), 20 kDa. Apart from being model proteins, these luminescent labels can show the chaperonin localization within the cell and its intermolecular interactions [29]. The constructed plasmids encoding the fusion proteins GroEL-EGFP and GroEL-GLuc were expressed in *Escherichia coli*. The GroEL-EGFP fusion proved the most informative. The expression of the plasmid encoding GroEL-EGFP alone does not result in the formation of a tetradecameric double-ring GroEL particle; the yielded product is seemingly monomeric GroEL-EGFP fusion with a molecular weight of about 90 kDa, as evaluated by size-exclusion chromatography. In contrast, when coexpressed with the plasmid producing excessive wild-type GroEL subunits, this plasmid provides

the full-size GroEL₁₄ particles with incorporated EGFP. Fluorescent microscopy shows that the GroEL₁₄-EGFP particles are evenly distributed inside the normally divided cells, while within abnormal gigantic nondivisible cells, they are concentrated mostly near the periplasm. The product of this coexpression was purified and analyzed by polyacrylamide gel electrophoresis (PAGE), fluorescence, absorption, transmission electron microscopy (TEM), and small-angle X-ray scattering (SAXS). It contains full-size GroEL₁₄ particles with incorporated EGFP (GroEL₁₄-EGFP particles). The amount of incorporated EGFP was estimated to be 1 per 12 ± 2 wild-type (WT) GroEL subunits, i.e., 1 subunit fused with EGFP in a tetradecameric GroEL₁₄ particle. The SAXS data and structural reconstitution of TEM images suggest the EGFP localization inside the GroEL inner cavity. The presence of a fluorescent protein in the tetradecameric GroEL₁₄ population allows for tracing its behavior by EGFP fluorescence and leads to the conclusion that tetradecameric GroEL₁₄-EGFP can interact with GroES and non-native proteins.

Using the same technique of coexpression in *E. coli* of two plasmids encoding the fusion GroEL-GLuc and the WT GroEL subunit, we obtained tetradecameric GroEL₁₄ with incorporated GLuc (GroEL₁₄-GLuc) and analyzed its binding to GroES and non-native proteins in both cell lysate and purified samples. Using BRET, the distance between the fluorescein-labeled non-native protein and the bioluminescent chromophore of GLuc incorporated into GroEL₁₄ was estimated as ~70 Å, which hints at the localization of the non-native protein bound mainly to the GLuc-free end of the GroEL₁₄-GLuc cylinder.

2. Results

2.1. The Analysis of Plasmid Expression Products

The basic condition for the successful *in vivo* incorporation of photoproteins into GroEL₁₄ tetradecameric quaternary structure is the coexpression of two plasmids. One of them encodes the WT GroEL subunit and possesses a high copyability while the other encodes the fusion GroEL-EGFP and displays a much lower copyability (see Materials and Methods (Section 4)). A schematic representation of these genetic constructs is shown in Figure 1a,b.

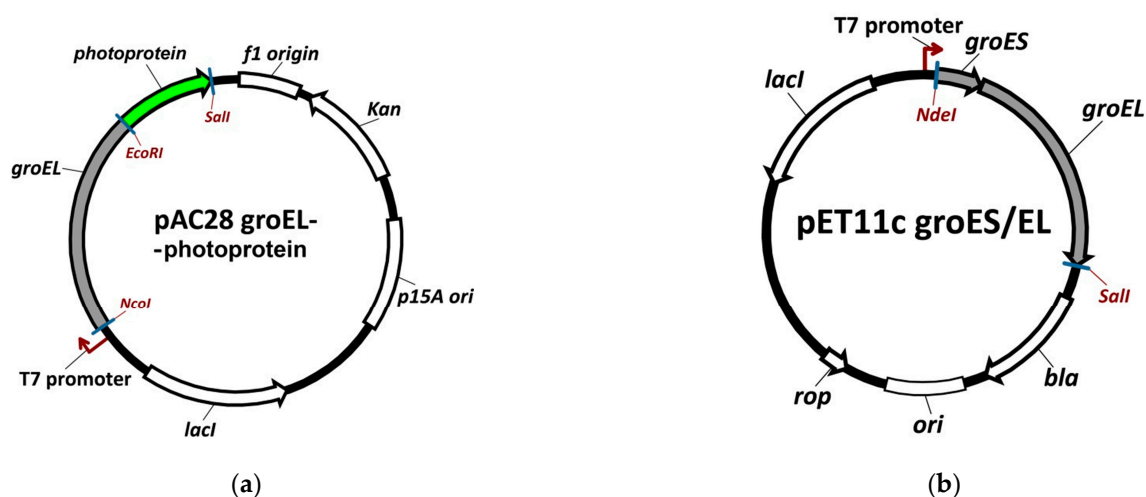


Figure 1. Cont.

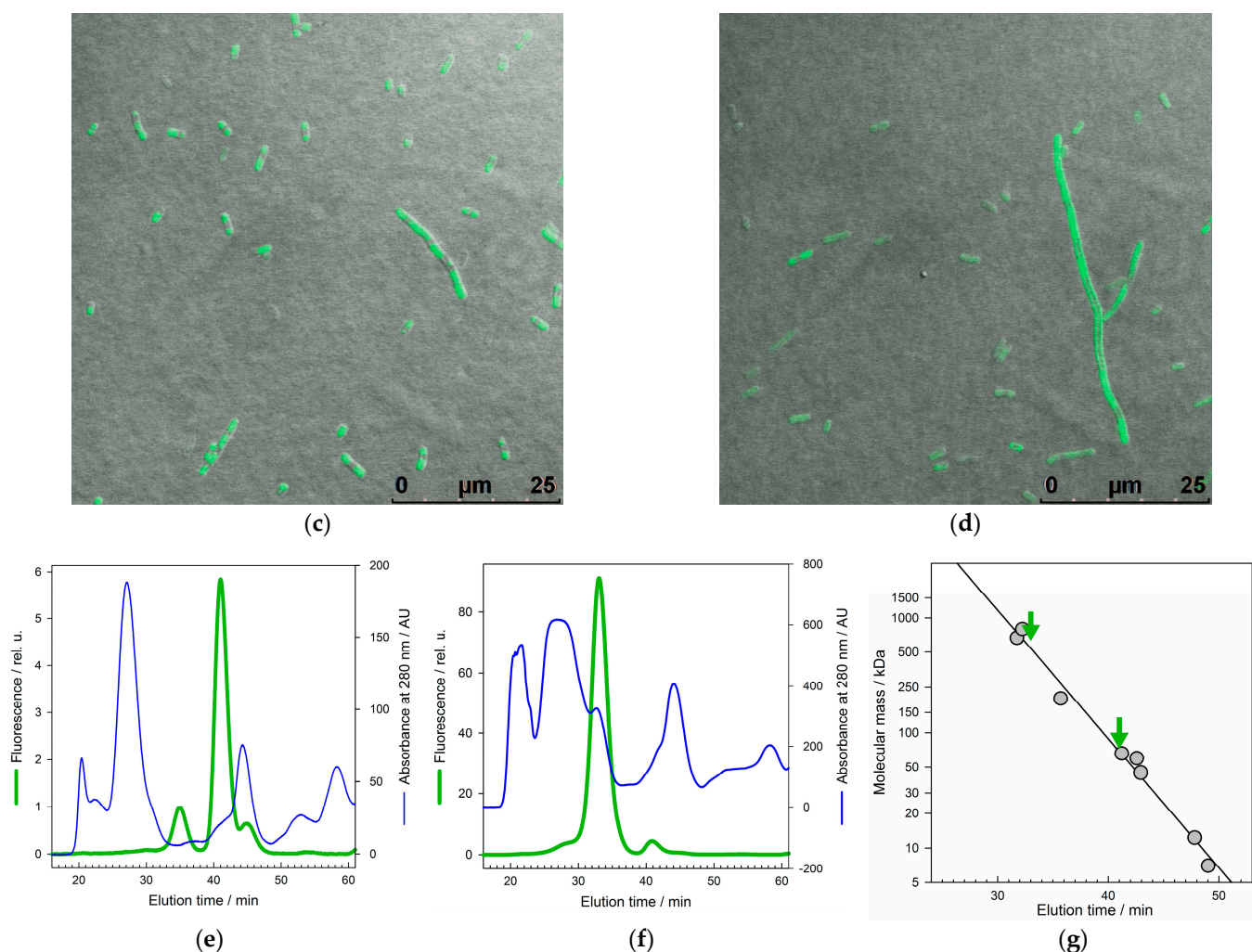


Figure 1. Incorporation of the photoprotein EGFP into the GroEL₁₄ structure: schematic representation of the genetic constructs encoding the GroEL subunit fused with photoprotein (a) and the WT groE operon (GroEL + GroES genes) of *E. coli* cells (b); fluorescent microscopy images of *E. coli* cells after the expression of pAC28 groEL-EGFP alone (c) and its coexpression with pET11c groES/EL (d); size-exclusion chromatography profiles of the corresponding cell lysates are shown in (e,f), and the column calibration is in (g); the green arrows indicate the elution times of monomeric GroEL₁-EGFP and oligomeric GroEL₁₄-EGFP. Abbreviations in the schemes (a,b) mean the following: pAC28 groEL-photoprotein and pET11c groES/EL are names of the constructed plasmids; *Kan* is the gene encoding resistance to kanamycin; *p15A ori* is the origin of replication p15A; *lacI* is the *lac* repressor; *bla* is the beta-lactamase gene; *ori* is the origin of replication ColE1; *rop* is the gene of Rop protein; *NcoI*, *EcoRI*, *Sall*, and *NdeI* are restriction sites.

Figure 1c,d shows fluorescent microscopy images of *E. coli* cells after the expression of pAC28 groEL-EGFP alone and its coexpression with pET11c groES/EL. Size-exclusion chromatography profiles of the corresponding soluble fractions of cell lysate are presented in Figure 1e,f. These data are evidence for the following. Firstly, the folding of EGFP as a part of GroEL-EGFP results in its physiological intrinsic green fluorescence. Secondly, there is an even diffuse distribution of GroEL-EGFP within normally divided cells and uneven distribution within abnormal nondivisible cells where no fluorescence is observed within the central part of the gigantic cells. Thirdly, the expression of pAC28 groEL-EGFP encoding GroEL-EGFP alone results in producing mostly monomeric GroEL₁-EGFP fusion (~90 kDa), whereas the product of its coexpression with pET11c groES/EL encoding the groE operon of wild type is the tetradecameric double-ring GroEL₁₄-EGFP (~800 kDa).

Note that nondivisible gigantic cells are observed only in the case of the coexpression, i.e., when full-size tetradecameric GroEL₁₄ particles are overproduced (Figure 1c,d).

The populations of GroEL₁₄-EGFP and GroEL₁-EGFP were purified (see Materials and Methods (Section 4)) to reveal some of their physicochemical properties. First, the amount of GroEL₁-EGFP fusion in the population of full-size tetradecameric GroEL₁₄-EGFP was estimated using SDS-PAGE and spectrophotometry (Figure 2). It appeared to be 1 fusion GroEL-EGFP subunit per 12 ± 2 WT subunits, as follows from the intensity of electrophoretic bands corresponding to the Coomassie-stained WT GroEL (~60 kDa) and GroEL-EGFP (~90 kDa) (Figure 2a) and from the spectrophotometric analysis (Figure 2b).

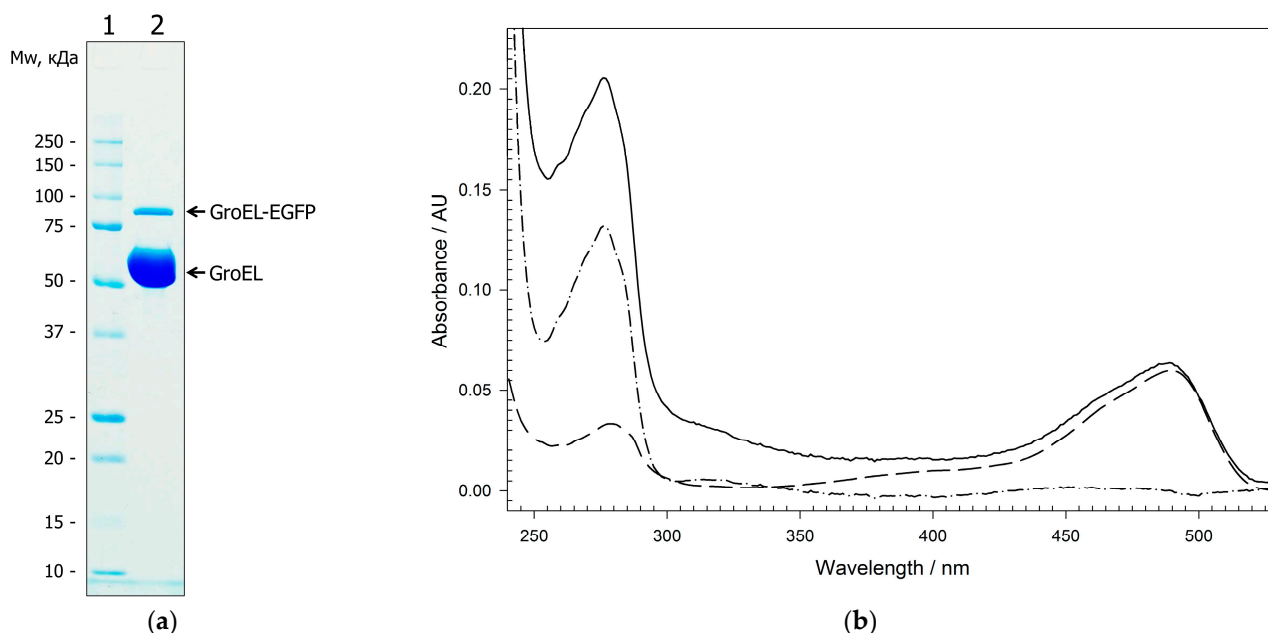


Figure 2. An estimation of the amount of fusion protein GroEL₁-EGFP incorporated in tetradecamer GroEL₁₄ particle: (a) SDS-PAGE electrophoresis of the GroEL₁₄-EGFP population (Lane 2). The intensity of the WT GroEL subunit band is 9.69 relative units while that of the fusion GroEL₁-EGFP is 1. Molecular-weight markers (Lane 1). (b) Absorption spectra of the GroEL₁₄-EGFP population (black solid line), monomeric fusion GroEL₁-EGFP (black dashed line, absorbance at 489 nm is $A_{489\text{nm}} = 0.06$ absorbance units (AU), concentration of the protein is $C = 1.07 \mu\text{M}$). The absorption spectrum of WT GroEL₁₄ subunits (black dashed-dot line) was obtained by subtraction of the GroEL₁-EGFP spectrum from the spectrum of the GroEL₁₄-EGFP population after their normalization at 499 nm (EGFP absorption) with a negligible contribution of the light scattering, and by the correction for light scattering, $A_{280\text{nm}} = 0.12$ AU, $C = 14.3 \mu\text{M}$.

2.2. Physicochemical Properties of GroEL₁₄ with Incorporated EGFP

Figure 3 shows SAXS patterns and Guinier plots of WT GroEL₁₄ and GroEL₁₄-EGFP populations purified after expression of pET11c groES/EL alone and with pAC28 GroELgroEL-EGFP. Although these patterns are very similar, which implies the similarity of the protein quaternary structures, there are two distinctions. One is a more pronounced minimum in the SAXS pattern at $0.055 (\text{\AA}^{-1})$ of the population with EGFP incorporated. The other is a decrease in the radius of gyration (Rg) by 5\AA for the GroEL₁₄-EGFP as compared to GroEL₁₄. The construction of the SAXS pattern in the form of a Guinier plot allows us to evaluate the radius of gyration and molecular mass of the proteins studied [30]. The radius of gyration is determined using the tangent of the slant of the linear part of the Guinier plot [30]. In our case, the linear part of the Guinier plot is within the scattering vector (h) range of 0.009 to 0.018\AA^{-1} (Figure 3b,d). The extrapolation of the Guinier plot to zero of the scattering vector (h) allows determining the scattering intensity at the zero-scattering angle. This value contains the information about the molecular mass of the

proteins studied, if the correction for protein concentration has been made, and if some standard with known molecular mass was used [30]. It is interesting that after correction on the protein concentration, the $I(0)$ values for both populations are close to each other, hinting at the proximity of the molecular weights of these proteins. The other possibility to estimate independently the Guinier parameters and molecular weight of the proteins studied is represented in the recent works of Piiadov et al. [31,32]. We uploaded our SAXS data to the online calculator described in these works and obtained the following results. SAXS pattern of WT GroEL₁₄ population: Guinier limits: from 0.007 Å⁻¹ to 0.019 Å⁻¹; Rg = 68 Å; integration limit $h \cdot R_g = 1.300$ (using 8/Rg); found molecular weight: 1400 kDa. SAXS pattern of GroEL₁₄-EGFP population: Guinier limits: from 0.007 Å⁻¹ to 0.020 Å⁻¹; Rg = 63 Å; integration limit $h \cdot R_g = 1.286$ (using 8/Rg); found molecular weight: 974 kDa. The Rg decrease may be caused by both the EGFP incorporation into the GroEL₁₄ inner cavity because it reflects an increase in the protein density arising with proximity to the protein center of mass and the decrease in the protein hydrodynamic size. Unfortunately, the molecular weight of the protein studied is closely related to the radius of gyration in the approach proposed by Piiadov et al. [31,32], and the reason for the Rg value change is not taken into account. Nevertheless, within the error of the method [31], the molecular weight estimated seems to be real for GroEL₁₄. The SAXS pattern of GroEL at 0.055 (Å⁻¹) of the scattering vector is mainly sensitive to an interring distance (our unpublished data).

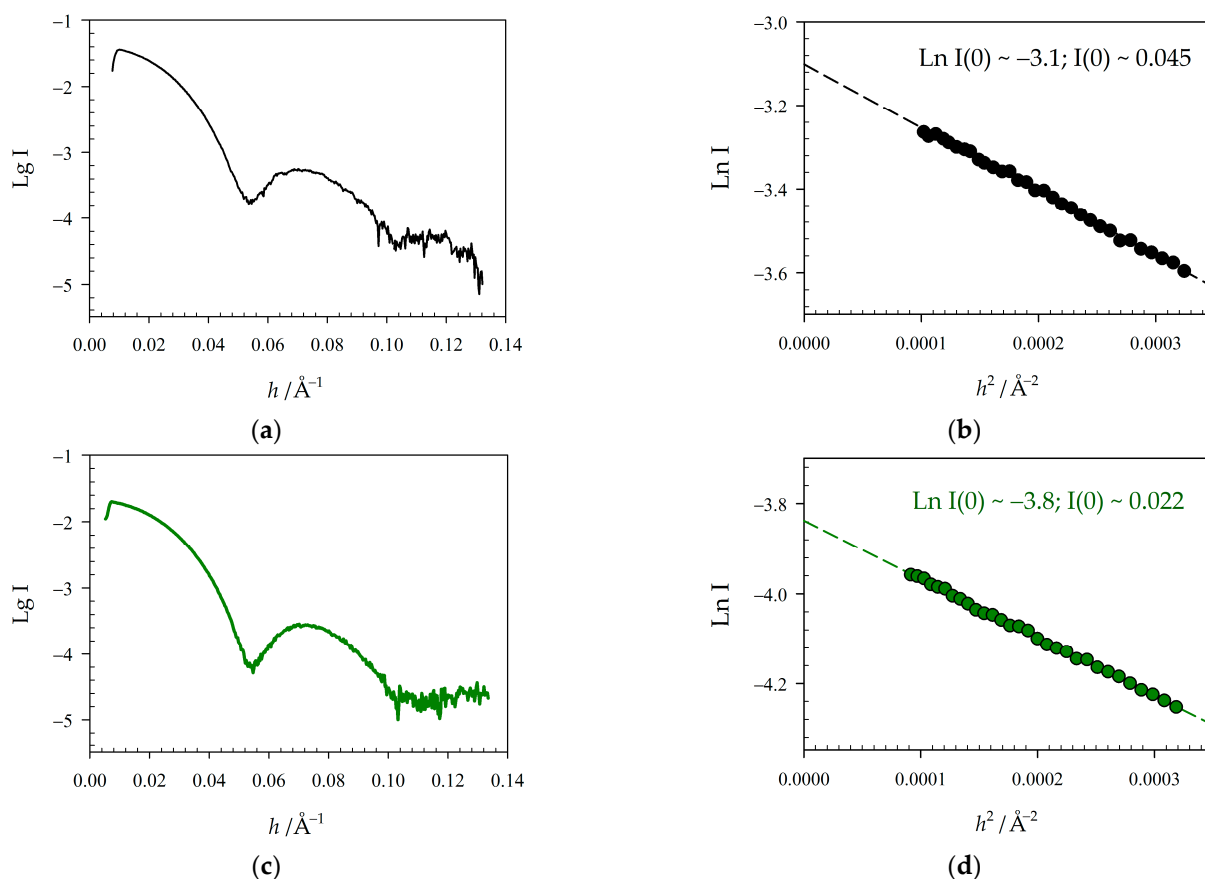


Figure 3. SAXS pattern of WT GroEL₁₄ population of 5 mg/mL (a, indicated in black) and GroEL₁₄-EGFP population of 2.5 mg/mL (c, indicated in green); (b,d) corresponding Guinier plots; scattering vector $h = 4 \times (\pi/\lambda) \times \sin(\theta)$, where 2θ —scattering angle and λ —wavelength; I —X-ray intensity. Radius gyration $R_g = 67.7 \pm 0.2$ (Å) for WT GroEL₁₄ and 62.5 ± 0.2 (Å) for GroEL₁₄-EGFP. Buffer: 20 mM Tris-HCl pH 7.6, 100 mM KCl, 10 mM MgCl₂.

The transmission electron microscopy fields of vision of both products are shown in Figure 4. One looks like the known side and top images of the WT GroEL₁₄ particles [8,13,33]

(Figure 4a,c). The images of GroEL₁₄-EGFP (Figure 4b,d) are different from those of the WT GroEL₁₄ due to a certain electron density inside the GroEL₁₄ inner cavity and perturbation in the region of the protein equatorial domains resulting in the absence of some interring distance which is clearly visible in WT GroEL₁₄ side view. The structural reconstructions of the images by the program EMAN2 [34] (see Materials and Methods (Section 4)) (Figure 4e,f) confirmed the presence of the EGFP fused part within the inner cavity of one ring of the tetradecameric GroEL₁₄ double-ring particle and decrease the interring distance in the case of the GroEL₁₄-EGFP population. The resolution of the models of GroEL₁₄ and GroEL₁₄-EGFP obtained after refinement was 20–21 Å and 22–26 Å correspondingly.

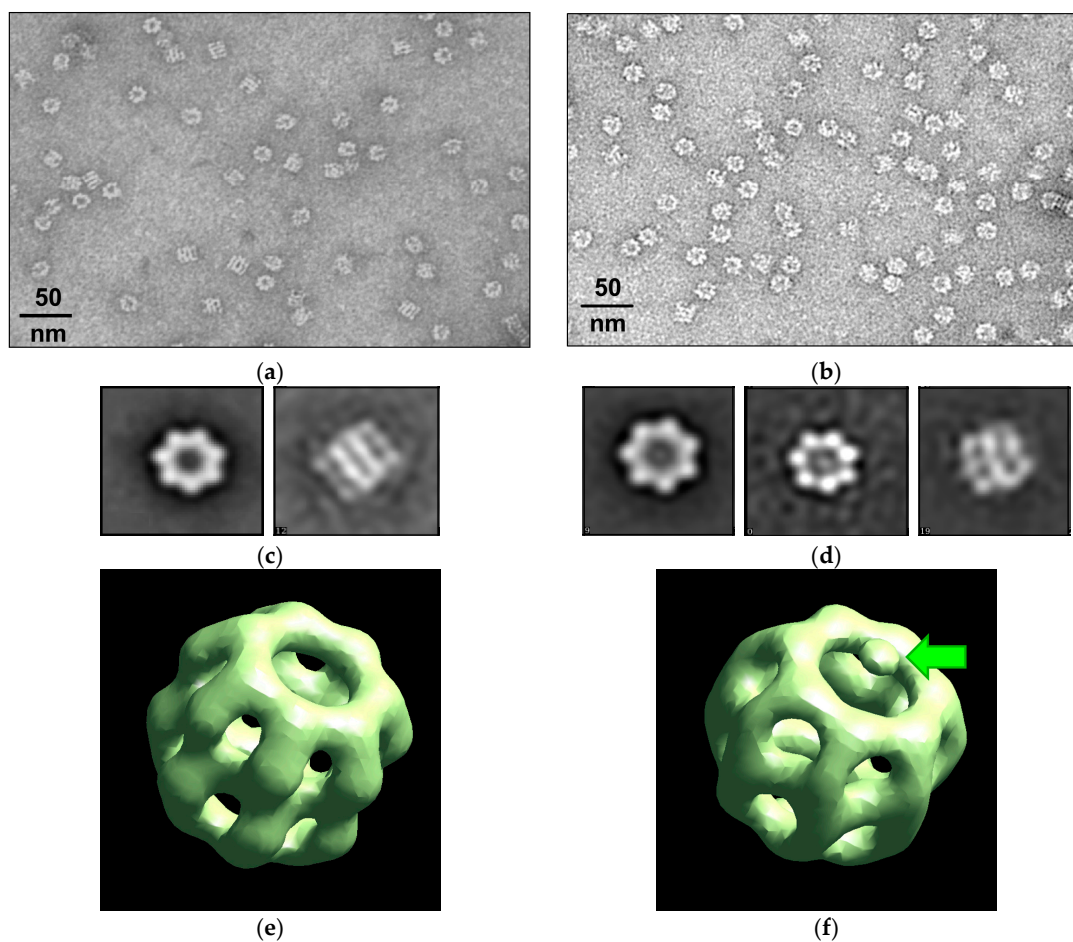


Figure 4. The reconstruction of the GroEL₁₄ and GroEL₁₄-EGFP spatial structures using their TEM images: the field and identified averaged top and side views of GroEL₁₄ (a,c) and GroEL₁₄-EGFP (b,d); the respective reconstructions (e,f). The green arrow indicates the center of the EGFP position in the reconstruction.

To verify the ability of GroEL₁₄-EGFP to bind to GroES and denatured proteins, we used nondenaturing PAGE and affinity chromatography based on denatured lysozyme (see [35]). Figure 5a presents the nondenaturing PAGE of the coexpression product GroEL₁₄-EGFP without and with GroES and Mg-ADP and shows protein electrophoretic bands detected by Coomassie staining and fluorescence (see Materials and Methods (Section 4)). As seen, in the presence of GroES and Mg-ADP, the mobility of the part of the protein band is noticeably retarded in the case of both Coomassie staining and fluorescence (Figure 5a). It means that GroEL₁₄-EGFP can bind to GroES. Moreover, GroEL₁₄-EGFP can tightly interact with denatured lysozyme (Figure 5b). Thus, the GroEL₁₄ particles with EGFP incorporated in their inner cavity retain the main chaperonin functions, i.e., the ability to bind non-native proteins and GroES.

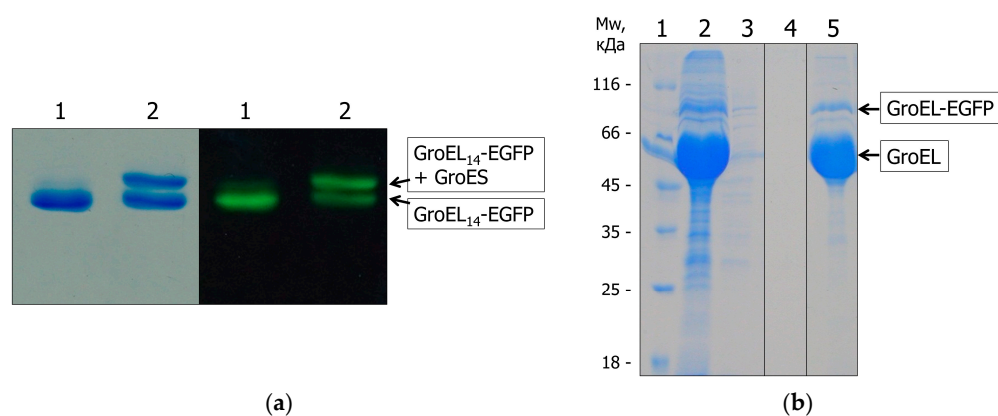


Figure 5. Binding of purified GroEL₁₄-EGFP to GroES (a); binding of GroEL₁₄-EGFP from cell extract (coexpression, see Materials and Methods (Section 4)) to denatured lysozyme (b). (a) Nondenaturing PAGE in the presence of Mg-ADP without GroES (Lane 1) and after incubation with GroES at the 1:5 molar ratio (Lane 2), as detected by Coomassie staining (left panel) and EGFP fluorescence (right panel) in the same electrophoretic gel; (b) SDS-PAGE of the results of affinity chromatography based on denatured lysozyme of the cell extract (coexpression): Lane 1, molecular-weight markers; Lane 2, loading; Lane 3, breakthrough; Lane 4, washing; Lane 5, elution by 6 M urea. Three lanes are three parts of the same gel.

The same technology, i.e., coexpression of two plasmids encoding the GroEL subunit fused with photoprotein and the wild-type subunit, was applied to incorporate another photoprotein, luciferase of *Gaussia princeps*, into the GroEL₁₄ particle.

2.3. Physicochemical Properties of the GroEL₁₄ Particle with Incorporated GLuc

Figure 6 shows the bioluminescence spectrum of *E. coli* cells after coexpression of the plasmids encoding GroEL fused with GLuc and WT GroEL (Figure 6a), and non-denaturing PAGE of soluble fractions of their lysates (Figure 6b) (see Materials and Methods (Section 4)). The bioluminescence spectrum (Figure 6a) confirms that the luciferase is folded into a physiologically active conformation after biosynthesis in the cell as fused with the GroEL subunit. The electrophoretic mobility of the bioluminescent protein bands corresponds either to the mobility of full-size GroEL₁₄-GLuc or to that of the complex of GroEL₁₄-GLuc with endogenous GroES (Figure 6b).

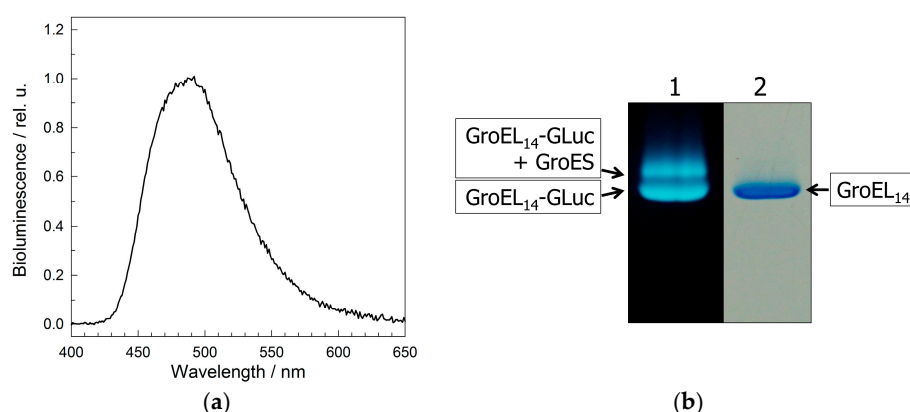


Figure 6. Physicochemical properties of GroEL₁₄ with incorporated *Gaussia princeps* luciferase (GroEL₁₄-GLuc): (a) the bioluminescence spectrum of cells after coexpression of pAC28 groEL-Luc and pET11c groES/EL; (b) non-denaturing PAGE of the cell lysate in the presence of Mg-ADP (Lane 1) and purified GroEL₁₄ (Lane 2). Protein band visualization by bioluminescence (Lane 1) and Coomassie staining (Lane 2).

To study the interaction of GroEL₁₄-GLuc with denatured proteins, the coexpression product was purified using the standard technique for GroEL purification [33,36]. Figure 7 shows the GroEL₁₄-GLuc bioluminescence spectra in the absence and presence of some fluorescein-labeled denatured proteins (see Materials and Methods (Section 4)). As seen, in the presence of fluorescein-labeled non-native proteins, the bioluminescence spectrum contains two components: bioluminescence of GroEL₁₄-GLuc and emission of the fluorescein label attached to the denatured protein. The fluorescein emission component is likely induced by the bioluminescence resonance energy transfer from GroEL₁₄-GLuc to the fluorescein-labeled denatured protein. The distance between the donor (GLuc) and acceptor (fluorescein) chromophores was estimated as $70 \pm 2 \text{ \AA}$, according to our method developed previously [37]. Thus, the full-size GroEL₁₄ particles with incorporated EGFP or GLuc can bind GroES and denatured proteins, thereby displaying the intrinsic chaperonin properties.

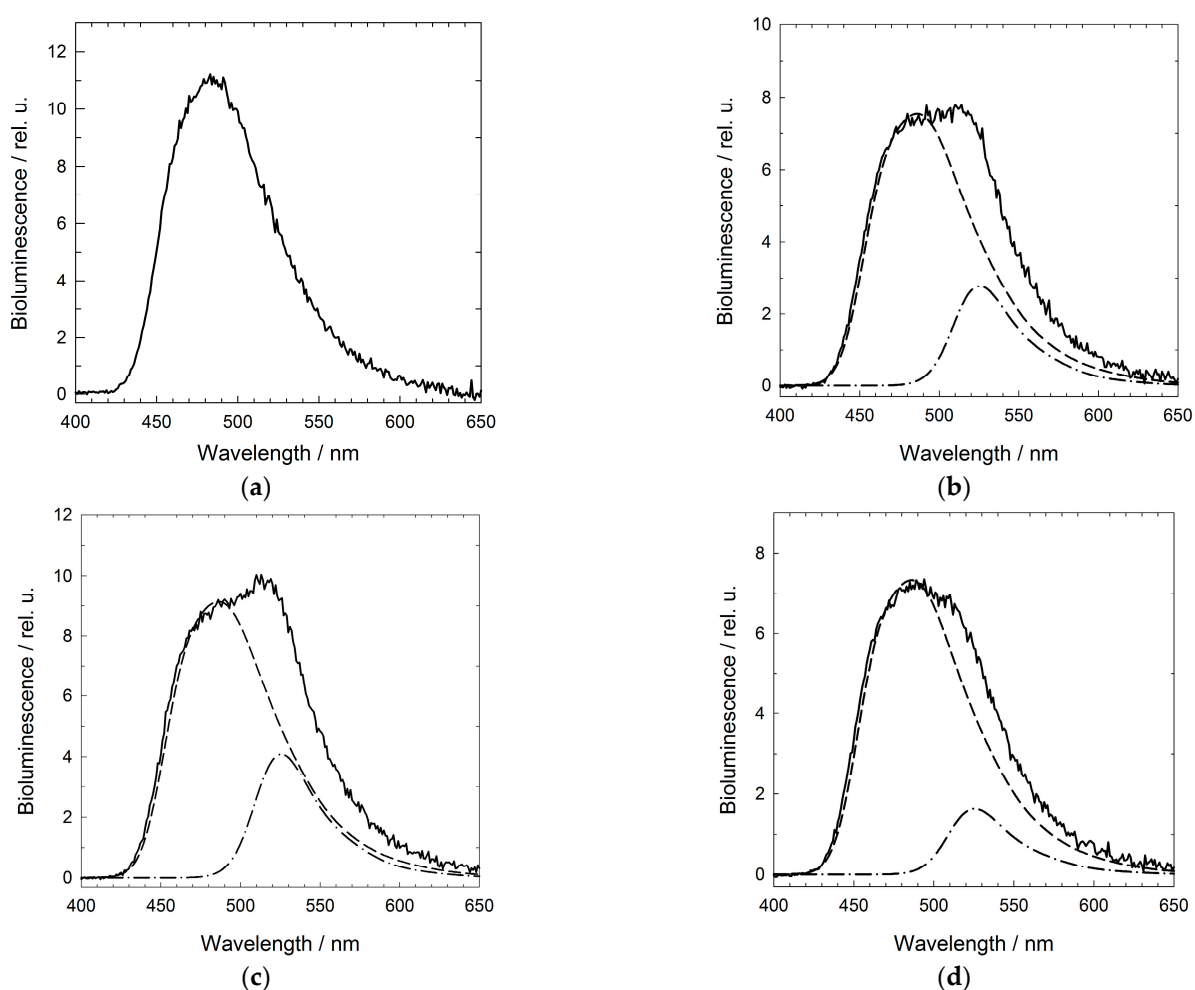


Figure 7. The interaction of purified GroEL₁₄-GLuc with fluorescein-labeled denatured proteins monitored by BRET: the bioluminescence spectra of GroEL₁₄-GLuc in the absence of denatured proteins (a) and in the presence of denatured lysozyme (b), α -lactalbumin (c), and malate dehydrogenase (d). The dashed lines show the contribution of bioluminescence to the spectrum; the dashed-dot lines are the contribution of BRET-induced fluorescein fluorescence.

3. Discussion

In this work, the key point is the proposed simple technique of incorporation of a photoprotein or any other protein of interest into the internal cavity of GroEL without significantly affecting its oligomeric structure and main functional properties, i.e., the ability

to bind the cochaperonin GroES and non-native proteins. This technique is based on the coexpression of two plasmids. One of them encodes the GroEL subunit fused with a protein of interest of appropriate size to fit the GroEL inner cavity (≤ 30 kDa), while the other encodes WT GroEL. These genetic constructs provide the excess of WT GroEL over that of the GroEL-fused protein of interest during the GroEL₁₄ assembly in vivo, which allows the spontaneous incorporation of a GroEL-fused protein molecule into the chaperonin inner cavity formed by the WT subunits. A disadvantage of this technique is the inability to incorporate more than one alien protein molecule into the tetradecameric GroEL₁₄ particle, i.e., only one ring of GroEL₁₄ can be occupied with an alien protein (Figures 2 and 4). GroEL crystal structure allows fitting EGFP into the inner cavity of the chaperonin without essential disruption of its quaternary structure (Figure 8). Nevertheless, it draws attention to the reduction of the interring distance that follows from the structural reconstruction of TEM images (Figure 4).

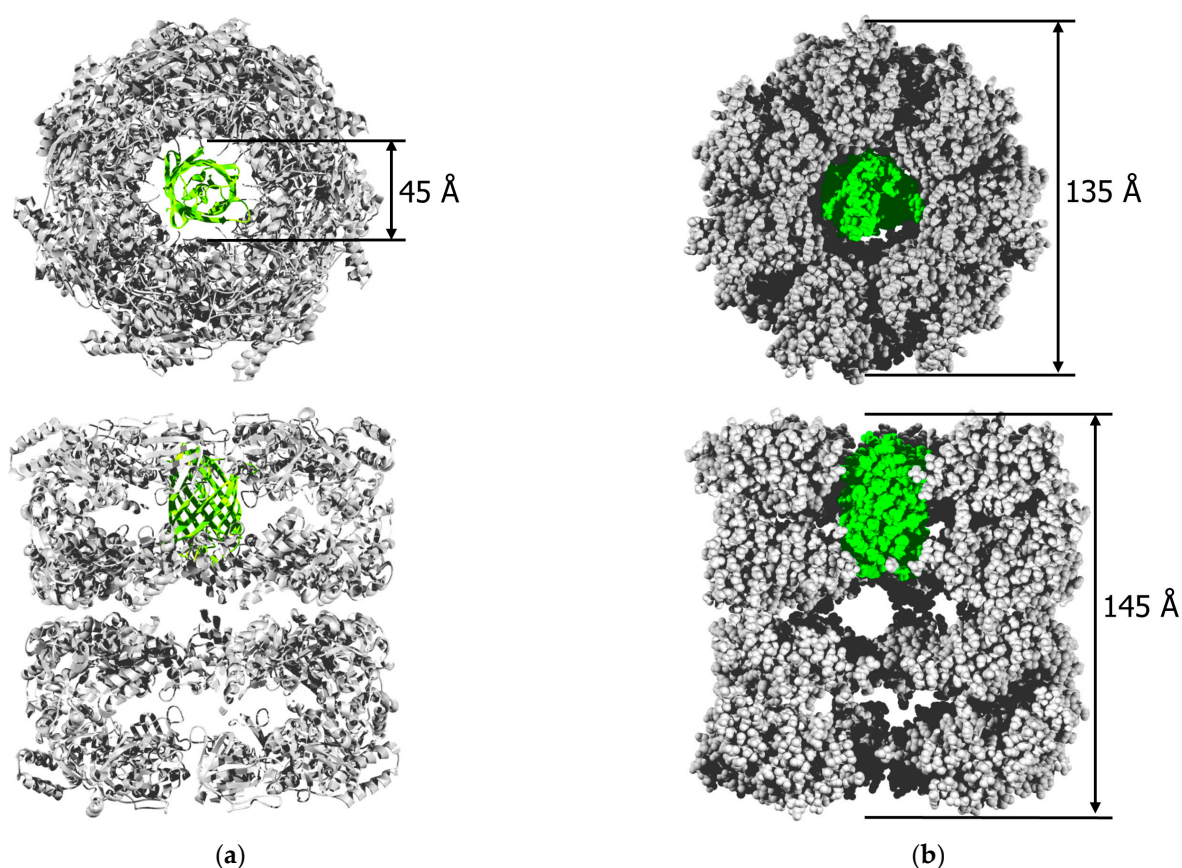


Figure 8. A model of GroEL₁₄ with EGFP incorporated into the inner cavity of one of the protein rings. (a) Ribbon view from top and side with three front subunits deleted; (b) space-fill view from top and side with three front subunits deleted. GroEL is in gray, and EGFP is in green. Structures used in modeling are from PDB ID 1OEL for GroEL [38] and PDB ID 2Y0G for EGFP [39]; the presentation was composed using SPDBViewer 4.1.0 software (developed by Nicolas Guex, Geneva, Switzerland) [40], and POV-Ray 3.7.0 software (Persistence of Vision Raytracer Pty. Ltd., Williamstown, Victoria, Australia).

The reason for such selectivity requires further research. In principle, the yield of the GroEL subunit fused with a photoprotein can be increased by using genetic constructs with promoters controlled by, e.g., arabinose, to adjust the biosynthesis level of GroEL fused with the protein of interest to that of WT GroEL. Nevertheless, the distance between GLuc and fluorescein-labeled denatured proteins was estimated from BRET to be $70 \text{ \AA} \pm 2 \text{ \AA}$. This hints that the binding of denatured proteins occurs mainly at the ring opposite to

the one occupied by GLuc (Figure 7). It is possible that the protein located in the inner cavity of GroEL creates some steric restrictions on the binding of denatured protein in this cavity. The fluorescence microscopy of *E. coli* cells after coexpression of two plasmids, one encoding WT GroEL and the other for EGFP fusion, shows the uneven distribution of GroEL₁₄-EGFP within nondivisible cells, while in normally divided cells, its distribution is diffused (Figure 1). This phenomenon is of interest and requires a special study. It is possibly caused by the interaction of oversynthesized full-size GroEL₁₄-EGFP with cell division proteins, e.g., FtsZ [41], and inhibition of cell division. The presence of EGFP in GroEL provides information about the size of molecules directly in the cell lysate without their purification (Figure 1). GroEL₁₄-EGFP particles have a decreased radius of gyration as compared to GroEL₁₄ particles (Figure 3), thereby suggesting EGFP localization inside the GroEL₁₄ cavity and the decrease in the protein interring distance. The structural reconstruction of GroEL₁₄ and GroEL₁₄-EGFP using relevant electron microscopy images supports this conclusion. GroEL₁₄-EGFP was tested for the ability to interact with the cochaperonin GroES and a denatured protein, in our case, lysozyme lacking disulfide bonds [35]. The test confirmed that the GroEL₁₄-EGFP particle retains its main functional features—the interaction with GroES and the denatured protein. Using the same technique of coexpression, the smaller photoprotein, *Gaussia princeps* luciferase of about 20 kDa, was apparently incorporated into the inner cavity of one GroEL ring. The protein GroEL₁₄-GLuc exhibits specific GLuc bioluminescence and interacts with endogenous GroES from the cell lysate, as shown by nondenaturing electrophoresis, followed by bioluminescence recording of coelenterazine-treated gel, which is very useful in studying heterogeneous solutions. Thus, our finding is that the incorporation of proteins of appropriate size into the GroEL₁₄ inner cavity can spontaneously occur *in vivo* resulting from the coexpression of two plasmids one of which encodes the GroEL subunit fused with the protein of interest while the other encodes WT GroEL, with the excess of the latter over the former. This technique can be used in biotechnology and biomedicine.

4. Materials and Methods

4.1. Chemicals and Related Enzymes

In the present work, the following reagents were used: HCl, NaOH, NaCl (Reachem, Moscow, Russia); acrylamide, β -mercaptoethanol, molecular weight protein markers, ammonium sulfate, SDS (Sigma-Aldrich, St. Louis, MO, USA); buffer components HEPES, KCl, DTT, MgCl₂, CaCl₂, Na₂HPO₄, NaH₂PO₄ (ICN Biomedicals, Costa Mesa, CA, USA); coelenterazine (Intrinsic Bioprobes, Tempe, AZ, USA). Substrate proteins for GroEL₁₄: lysozyme, α -lactalbumin, and malate dehydrogenase were purchased from Sigma-Aldrich (St. Louis, MO, USA).

4.2. Bacterial Strains, Culture Conditions, and Enzymes

Escherichia coli strain DH5 α (Novagen, Madison, WI, USA) was used for DNA plasmid propagation, and *E. coli* strain BL21(DE3) (Novagen, Madison, WI, USA) was used for gene expression. *E. coli* cells were routinely grown in lysogeny broth (LB) [42] at 37 °C. For the selection and maintenance of the plasmids, LB medium was supplemented with ampicillin at 100 $\mu\text{g mL}^{-1}$ and kanamycin at 20 $\mu\text{g mL}^{-1}$. Restriction enzymes and nucleases, T4 ligase, dNTPs, and isopropyl β -D-1-thiogalactopyranoside (IPTG) were from Thermo Fisher Scientific (Vilnius, Lithuania). Pfu Turbo high-fidelity DNA polymerase was from Alfa Ferment (Moscow, Russia). All enzymes were used as recommended by the suppliers.

4.3. Genetic Manipulations

Standard procedures were used for DNA restriction, ligation, gel electrophoresis, and transformation of *E. coli* [42]. Plasmid DNA was purified using QIAprep Spin Miniprep Kit (Qiagen, Hilden, Germany). QIAquick gel extraction and QIAquick PCR purification kits (Qiagen, Hilden, Germany) were used for DNA isolation from agarose gels and purification of PCR products.

To construct fused in frame *groEL* with EGFP or luciferase GLuc from *Gaussia princeps* genes, the low copy (~ 10 copies per cell) expression plasmid pAC28 [43] was used. The *groEL* without stop codon was amplified with the pair of primers 5'-TTCCATGGCAGCTAAAGACGTAAAATTC-3' and 5'-TTGAATTCCGGCATCATGCCGCCCATG-3' (restriction sites are underlined) and cloned into NcoI/EcoRI sites of pAC28 to give pAC28 *groEL*. The EGFP was amplified using the 5'-TTGAATTCCGGTGTGAGCAAGGGCGAGGAG-3' and 5'-TTGTCGACTTACTTGTACAGCTCGTCCATGC-3' primers. The DNA fragment containing the GLuc gene without the 17 a.a. signal peptide was amplified with the 5'-TTGAATTCCGGGAAACCAACTGAAAACAATGAAGAT-3' and 5'-TTGTCGACTTAATCAACACCGCACCCCT-3' primers. The PCR products were cloned independently into the pAC28 *groEL* plasmid at the EcoRI/SalI sites. The resultant plasmids allow producing fused proteins with a tetra-peptide linker, PEFG, between GroEL and EGFP or GLuc.

The recombinant plasmid containing *groES-groEL* operon was constructed as follows. The DNA fragment containing *groES-groEL* operon was amplified using the 5'-TTATTTTCATATGAATATTCGTCCATTGCATG-3' and 5'-TTGTCGACTTACATCATGCCGCCCAT-3 primers, respectively, and pACYC184 *groES-groEL* (gift of A.S. Girshovich [33]) as a template. The resulting amplicon was cloned into the NdeI/SalI sites of medium copy number pET11cjo vector (gift of H.J. Khackmuss, Stuttgart University, Stuttgart, Germany) to create pET *groES-groEL* compatible with pAC28. The constructed plasmids were employed for the coexpression in *E. coli* BL21(DE3) cells.

4.4. Protein Purification and Labeling

GroEL, both of wild type and with photoproteins incorporated, as well as GroES, were isolated using standard published protocols [33].

To prepare the proteins labeled with fluorescein, their 5–10 mg/mL solutions in 0.2 M NaHCO₃, pH 8.4, were incubated with a 5-fold molar excess of 5- (and 6)-carboxyfluorescein succinimidyl ester “mixed isomers” (Invitrogen, Waltham, MA, USA) at intensive mixing with Heidolph Reax top (Heidolph Instruments, Schwabach, Germany) for 1 h at room temperature. The reaction was stopped by the addition of 1 M Tris-HCl, pH 7.6, up to 10 mM. Nonbound labels were removed using a G25 gel chromatographic column PD10. The labeled proteins were fractionated additionally with DEAE-Toyo Pearl (HαLA) or CM-Toyo Pearl (lysozyme and MDH) to separate the populations with different amounts of the labels. After that, each fraction underwent gel filtration with a Sephacryl S100 1.6 × 60 cm column in 20 mM NaHCO₃, pH 8.4, to achieve the most homogeneous labeled protein. The concentration of fluorescein-labeled proteins was determined spectrophotometrically after subtracting the contribution of the fluorescent label (using the known fluorescein extinction coefficient at 490 nm of 87,000 M⁻¹ cm⁻¹) and confirmed by SDS-PAGE densitometric analysis. The denatured states of lysozyme and α-lactalbumin were attained by reducing intermolecular disulfide bonds with DTT [35], while that of MDH was by dilution from 8 M urea solution.

4.5. Registration of Fluorescence and Bioluminescence in the Cells, Cell Extracts, Electrophoretic Gels, and Pure Protein Solutions

The aliquots of precipitate cells were resuspended in 80 μL of 20 mM Tris-HCl, pH 7.6, 150 mM NaCl up to OD_{590nm} = 0.25. To measure the bioluminescence spectra, 25 μM coelenterazine (CZ) was added to the cell suspension at mixing. Using a quartz cuvette 3 × 3 × 5 mm, 10 bioluminescence spectra of the solution were recorded with a Varian Cary Eclipse spectrofluorimeter (Palo Alto, CA, USA) in the mode “the lamp is off” within the wavelength region from 330 nm up to 730 nm. The spectra were corrected to the time-dependent decay of bioluminescence occurring due to coelenterazine consumption, its penetration into cells, etc., using the bioluminescence decrease at 470 nm and then averaged, followed by the resultant value correction for spectral sensitivity of the device [44]. Note that the time-dependent bioluminescence decrease in the case of *Gaussia princeps* luciferase

is not significant and occurs within 300 s by only 25%. The EGFP fluorescence spectra were recorded with excitation at 470 nm.

The same procedures were applied to record luminescence of cell lysates and purified proteins. To register EGFP fluorescence in the gel after nondenaturing PAGE of GroEL₁₄-EGFP fusions, the electrophoretic plates with the gel inside were photographed through an orange glass filter GS-20 (Krasnyj Gigant, Nikolsk, Russia) with the maximum transmission at the green region of the spectrum while illuminating the bottom and top with a group of blue LEDs arranged in a line. To register GLuc bioluminescence, one of two glass plates of electrophoretic gel was removed, and on the open side of the gel, 1 mL of 20 μM coelenterazine solution in 20 mM Tris-HCl, 100 mM KCl, and 10 mM MgCl₂ was evenly loaded. The plate was placed in a darkened box and photographed with a long exposure of 30 s.

The distances between fluorescein and GLuc chromophores attached to proteins were evaluated from BRET according to the published method [37].

The protein absorption spectra were recorded using a Cary 100 Bio spectrophotometer (Varian Medical Systems, Palo Alto, CA, USA). Protein concentrations were determined using molar extinction coefficients at 280 nm of 9080 M⁻¹ cm⁻¹ for WT GroEL₁₄ [45], at 280 nm of 1280 M⁻¹ cm⁻¹ for WT GroES₇ [45], and at 280 nm of 22,000 M⁻¹ cm⁻¹ and at 489 nm of 56,000 M⁻¹ cm⁻¹ for EGFP [46].

The size-exclusion chromatography was performed using a ProStar HPLC chromatograph (Varian Medical Systems, Palo Alto, CA, USA), a Superose 6 10/300 GL column, and a flow rate of 0.4 mL/min; the column was calibrated using the following proteins (from Gel Filtration Calibration Kit, Pharmacia, Uppsala, Sweden; Sigma-Aldrich, St. Louis, MO, USA): WT GroEL₁₄ (800 kDa), thyroglobulin (669 kDa), bovine serum albumin trimer (198 kDa), bovine serum albumin monomer (66 kDa), catalase monomer (60 kDa), ovalbumin (45 kDa), cytochrome *c* (12.3 kDa), insulin (7 kDa). The chromatographic profiles were simultaneously recorded by EGFP fluorescence with $\lambda_{\text{ex}} = 280$ nm, $\lambda_{\text{em}} = 515$ nm, and absorbance at 280 nm.

4.6. SAXS Measurements

X-ray solution scattering measurements were performed on the beam line BL-6A small-angle installation. A stable beam of photons with a wavelength of 1.503 Å was provided by a bent-crystal horizontally focusing monochromator and a vertically focusing mirror [47] of the Photon Factory, National Laboratory for High Energy Physics, Tsukuba, Japan. A camera with a 2.35 m sample-to-detector distance collected data in the range of the scattering vector (h) from 0.008 to 0.2 Å⁻¹. The background data for the buffer solvent were collected before or after data collection for the protein solution. The temperature was kept at 23 °C for all the measurements. The data were registered by the two-dimensional CCD X-ray detector PILATUS 100 K. For SAXS data integration and Guinier analysis ATSAS online 3.2.1 software (BioSAXS group, EMBL Hamburg, Germany) was used.

4.7. Transmission Electron Microscopy and Images Processing

Samples for electron microscopy (EM) studies were prepared according to the negative staining method. A copper 400-mesh grid (Electron Microscopy Science, Hatfield, PA, USA) coated with a formvar film (0.2% formvar solution in chloroform) was mounted on a sample drop (10 μL). After 5 min absorption, the grid with the preparation was negatively stained for 1.5–2.0 min with 1% (*w/v*) aqueous solution of uranyl acetate. The excess of the staining agent was removed with filter paper. The preparations were analyzed using a JEM-1200EX transmission electron microscope (JEOL, Ltd., Tokyo, Japan) at the accelerating voltage of 80 kV. Images were recorded on the Kodak electron image film (SO-163) at nominal magnification of 40,000.

Reference-free 2D classification, initial model building, 3D classification, 3D refinement, and CTF refinement were performed using the EMAN2.22 software package (Baylor College of Medicine, Houston, TX, USA) [34]. The EMAN2.22 software package is a broadly

based greyscale scientific image processing suite with a primary focus on processing data from transmission electron microscopes. Despite EMAN's original purpose was performing single particle reconstructions (3D volumetric models from 2D cryo-EM images) in this work we used this program for processing data from transmission electron microscopy images of negatively stained molecules WT GroEL₁₄ and GroEL₁₄-EGFP. Particles were manually picked by the e2boxer.py program from the software package EMAN2. A total number of 1262 particles for GroEL and 1586 particles for GroEL-EGFP were used to generate 32 class averages and to build the final 3D reconstruction. At modeling, we used only one limitation—conservation of C7 or D7 symmetry, i.e., both rings are identical. In the case of the removal of this limitation, the models were very distorted and wry.

4.8. Fluorescence Microscopy

To obtain the fluorescent microscopy images the sterile glass plates were coated with 1% agarose in deionized water and dried in ultraviolet light. Aliquots (5–10 µL) of the *E. coli* cells transformed by the recombinant plasmids were loaded on these plates, covered with cover glasses and immediately visualized with Leica TCS SP5 Confocal Microscopy System (Leica Microsystems, Wetzlar, Germany). The excitation wavelength of the argon laser was 488 nm, and luminescence was measured in the EGFP luminescence band (500–550 nm). The images were analyzed using the Leica Application Suite AF 2.6.3 program (Leica Microsystems, Wetzlar, Germany).

Author Contributions: Conceptualization, V.K. and G.S.; Data curation, V.M. and N.M.; Formal analysis, V.M., N.R., O.S. and A.T.; Investigation, V.M., N.M., N.R., O.S., A.T. and H.K.; Methodology, V.M., T.I., V.K. and G.S.; Project administration, G.S.; Resources, V.M., T.I., N.M., N.R. and H.K.; Software, V.M. and A.T.; Supervision, G.S.; Validation, V.M. and G.S.; Visualization, V.M., N.M., N.R., and O.S.; Writing—original draft, G.S.; Writing—review and editing, N.M. and G.S. All authors have read and agreed to the published version of the manuscript.

Funding: This research received no external funding.

Institutional Review Board Statement: Not applicable.

Informed Consent Statement: Not applicable.

Data Availability Statement: Not applicable.

Acknowledgments: The authors are grateful to Rogachevskii V.V. (Institute of Cell Biophysics, Russian Academy of Sciences, Pushchino, Moscow Region, Russia) for providing working time on the electron microscope and Serebrova E.V. (Institute of Protein Research, Russian Academy of Sciences, Pushchino, Moscow Region, Russia) for help in manuscript preparation. This work was partially performed using the Electron Microscopy Core Facilities and Optical Microscopy and Spectrophotometry Core Facility, ICB RAS, Federal Research Center “Pushchino Scientific Center for Biological Research of the Russian Academy of Sciences” (<http://www.cbp-rf.ru/cbp/670266/>; accessed on 16 January 2023).

Conflicts of Interest: The authors declare no conflict of interest.

Sample Availability: Samples of the mutant plasmids are available from the authors.

References

1. Hartl, F.U.; Hayer-Hartl, M. Molecular chaperones in the cytosol: From nascent chain to folded protein. *Science* **2002**, *295*, 1852–1858. [[CrossRef](#)]
2. Yoshida, T.; Kawaguchi, R.; Taguchi, H.; Yoshida, M.; Yasunaga, T.; Wakabayashi, T.; Yohda, M.; Maruyama, T. Archaeal group II chaperonin mediates protein folding in the cis-cavity without a detachable GroES-like co-chaperonin. *J. Mol. Biol.* **2002**, *315*, 73–85. [[CrossRef](#)]
3. Vilasi, S.; Bulone, D.; Caruso Bavisotto, C.; Campanella, C.; Marino Gammazza, A.; San Biagio, P.L.; Cappello, F.; de Macario, E.; Macario, A.J.L. Chaperonin of Group I: Oligomeric Spectrum and Biochemical and Biological Implications. *Front. Mol. Biosci.* **2018**, *4*, 99. [[CrossRef](#)]
4. Rebeaud, M.E.; Mallik, S.; Goloubinoff, P.; Tawfik, D.S. On the evolution of chaperones and cochaperones and the expansion of proteomes across the Tree of Life. *Proc. Natl. Acad. Sci. USA* **2021**, *118*, e2020885118. [[CrossRef](#)]

5. Horwich, A.L.; Fenton, W.A.; Chapman, E.; Farr, G.W. Two families of chaperonin: Physiology and mechanism. *Annu. Rev. Cell Dev. Biol.* **2007**, *23*, 115–145. [[CrossRef](#)]
6. Hartl, F.U.; Bracher, A.; Hayer-Hartl, M. Molecular chaperones in protein folding and proteostasis. *Nature* **2011**, *475*, 324–332. [[CrossRef](#)]
7. Saibil, H. Chaperone machines for protein folding, unfolding and disaggregation. *Nat. Rev. Mol. Cell Biol.* **2013**, *14*, 630–642. [[CrossRef](#)]
8. Braig, K.; Otwinowski, Z.; Hegde, R.; Boisvert, D.C.; Joachimiak, A.; Horwich, A.L.; Sigler, P.B. The crystal structure of the bacterial chaperonin GroEL at 2.8 Å. *Nature* **1994**, *371*, 578–586. [[CrossRef](#)]
9. Semenyuk, P.I.; Moiseenko, A.V.; Sokolova, O.S.; Muronetz, V.I.; Kurochkina, L.P. Structural and functional diversity of novel and known bacteriophage-encoded chaperonins. *Int. J. Biol. Macromol.* **2020**, *157*, 544–552. [[CrossRef](#)]
10. Qamra, R.; Mande, S.C. Crystal structure of the 65-kilodalton heat shock protein, chaperonin 60.2, of *Mycobacterium tuberculosis*. *J. Bacteriol.* **2004**, *186*, 8105–8113. [[CrossRef](#)]
11. Gruber, R.; Horovitz, A. Allosteric Mechanisms in Chaperonin Machines. *Chem. Rev.* **2016**, *116*, 6588–6606. [[CrossRef](#)]
12. Lorimer, G.H.; Fei, X.; Ye, X. The GroEL chaperonin: A protein machine with pistons driven by ATP binding and hydrolysis. *Philos. Trans. R. Soc. Lond. B. Biol. Sci.* **2018**, *373*, 20170179. [[CrossRef](#)]
13. Saibil, H.R.; Fenton, W.A.; Clare, D.K.; Horwich, A.L. Structure and Allostery of the Chaperonin GroEL. *J. Mol. Biol.* **2013**, *425*, 1476–1487. [[CrossRef](#)]
14. Fei, X.; Yang, D.; LaRonde-LeBlanc, N.; Lorimer, G.H. Crystal structure of a GroEL-ADP complex in the relaxed allosteric state at 2.7 Å resolution. *Proc. Natl. Acad. Sci. USA* **2013**, *110*, E2958–E2966. [[CrossRef](#)]
15. Bracher, A.; Starling-Windhof, A.; Hartl, F.U.; Hayer-Hartl, M. Crystal structure of a chaperone-bound assembly intermediate of form I Rubisco. *Nat. Struct. Mol. Biol.* **2011**, *18*, 875–880. [[CrossRef](#)]
16. Chen, L.; Sigler, P.B. The crystal structure of a GroEL/peptide complex: Plasticity as a basis for substrate diversity. *Cell* **1999**, *99*, 757–768. [[CrossRef](#)]
17. Chatellier, J.; Hill, F.; Fersht, A.R. From minichaperone to GroEL 2: Importance of avidity of the multisite ring structure. *J. Mol. Biol.* **2000**, *304*, 883–896. [[CrossRef](#)]
18. Yuan, Y.; Du, C.; Sun, C.; Zhu, J.; Wu, S.; Zhang, Y.; Ji, T.; Lei, J.; Yang, Y.; Gao, N.; et al. Chaperonin-GroEL as a Smart Hydrophobic Drug Delivery and Tumor Targeting Molecular Machine for Tumor Therapy. *Nano Lett.* **2018**, *18*, 921–928. [[CrossRef](#)]
19. Horwich, A.L.; Farr, G.W.; Fenton, W.A. GroEL–GroES-Mediated Protein Folding. *Chem. Rev.* **2006**, *106*, 1917–1930. [[CrossRef](#)]
20. O’Neil, P.T.; Machen, A.J.; Deatherage, B.C.; Trecuzzi, C.; Tischer, A.; Machha, V.R.; Auton, M.T.; Baldwin, M.R.; White, T.A.; Fisher, M.T. The Chaperonin GroEL: A Versatile Tool for Applied Biotechnology Platforms. *Front. Mol. Biosci.* **2018**, *5*, 46. [[CrossRef](#)]
21. Furutani, M.; Hata, J.-I.; Shomura, Y.; Itami, K.; Yoshida, T.; Izumoto, Y.; Togi, A.; Ideno, A.; Yasunaga, T.; Miki, K.; et al. An engineered chaperonin caging a guest protein: Structural insights and potential as a protein expression tool. *Protein Sci.* **2005**, *14*, 341–350. [[CrossRef](#)]
22. Yurkova, M.S.; Sadykhov, E.G.; Fedorov, A.N. Production of a toxic polypeptide as a fusion inside GroEL cavity. *Sci. Rep.* **2020**, *10*, 21024. [[CrossRef](#)]
23. Yurkova, M.S.; Fedorov, A.N. GroEL-A Versatile Chaperone for Engineering and a Plethora of Applications. *Biomolecules* **2022**, *12*, 607. [[CrossRef](#)]
24. Kyratsous, C.A.; Silverstein, S.J.; DeLong, C.R.; Panagiotidis, C.A. Chaperone-fusion expression plasmid vectors for improved solubility of recombinant proteins in *Escherichia coli*. *Gene* **2009**, *440*, 9–15. [[CrossRef](#)]
25. Chitradevi, S.T.S.; Kaur, G.; Sivaramakrishna, U.; Singh, D.; Bansal, A. Development of recombinant vaccine candidate molecule against Shigella infection. *Vaccine* **2016**, *34*, 5376–5383. [[CrossRef](#)]
26. Kyratsous, C.A.; Panagiotidis, C.A. Heat-Shock Protein Fusion Vectors for Improved Expression of Soluble Recombinant Proteins in *Escherichia coli* BT—Recombinant Gene Expression. In *Recombinant Gene Expression*; Lorence, A., Ed.; Humana Press: Totowa, NJ, USA, 2012; pp. 109–129. ISBN 978-1-61779-433-9.
27. Yurkova, M.S.; Savvin, O.I.; Zenin, V.A.; Fedorov, A.N. Design and Characterization of a Methionineless Variant of Thermostable Chaperon GroEL from *Thermus thermophilus*. *Appl. Biochem. Microbiol.* **2019**, *55*, 112–116. [[CrossRef](#)]
28. Zenin, V.; Yurkova, M.; Tsedilin, A.; Fedorov, A. Enfuvirtide biosynthesis in thermostable chaperone-based fusion. *Biotechnol. Rep.* **2022**, *35*, e00734. [[CrossRef](#)]
29. Charbon, G.; Wang, J.; Brustad, E.; Schultz, P.G.; Horwich, A.L.; Jacobs-Wagner, C.; Chapman, E. Localization of GroEL determined by in vivo incorporation of a fluorescent amino acid. *Bioorg. Med. Chem. Lett.* **2011**, *21*, 6067–6070. [[CrossRef](#)]
30. Glatter, O.; Kratky, O. *Small Angle X-ray Scattering*; Kratky, O., Glatter, O., Eds.; Academic Press: London, UK, 1982; ISBN 0122862805.
31. Piiadov, V.; Ares de Araújo, E.; Oliveira Neto, M.; Craievich, A.F.; Polikarpov, I. SAXSMoW 2.0: Online calculator of the molecular weight of proteins in dilute solution from experimental SAXS data measured on a relative scale. *Protein Sci.* **2019**, *28*, 454–463. [[CrossRef](#)]
32. de Oliveira Neto, M.; de Freitas Fernandes, A.; Piiadov, V.; Craievich, A.F.; de Araújo, E.A.; Polikarpov, I. SAXSMoW 3.0: New advances in the determination of the molecular weight of proteins in dilute solutions from SAXS intensity data on a relative scale. *Protein Sci.* **2022**, *31*, 251–258. [[CrossRef](#)]

33. Lissin, N.M.; Venyaminov, S.Y.; Girshovich, A.S. (Mg-ATP)-dependent self-assembly of molecular chaperone GroEL. *Nature* **1990**, *348*, 339–342. [[CrossRef](#)]
34. Bell, J.M.; Chen, M.; Baldwin, P.R.; Ludtke, S.J. High resolution single particle refinement in EMAN2.1. *Methods* **2016**, *100*, 25–34. [[CrossRef](#)] [[PubMed](#)]
35. Marchenko, N.Y.; Sikorskaya, E.V.; Marchenkov, V.V.; Kashparov, I.A.; Semisotnov, G.V. Affinity chromatography of chaperones based on denatured proteins: Analysis of cell lysates of different origin. *Protein Expr. Purif.* **2016**, *119*, 117–123. [[CrossRef](#)] [[PubMed](#)]
36. Marchenkov, V.; Gorokhovatsky, A.; Marchenko, N.; Ivashina, T.; Semisotnov, G. Back to GroEL-assisted protein folding: GroES binding-induced displacement of denatured proteins from GroEL to bulk solution. *Biomolecules* **2020**, *10*, 162. [[CrossRef](#)]
37. Marchenkov, V.; Ivashina, T.; Marchenko, N.; Ksenzenko, V.; Semisotnov, G. Bioluminescence Resonance Energy Transfer (BRET) Allows Monitoring the Barnase-Barstar Complex In Vivo. *Biophysica* **2022**, *2*, 7. [[CrossRef](#)]
38. Braig, K.; Adams, P.D.; Brünger, A.T. Conformational variability in the refined structure of the chaperonin groel at 2.8 Å resolution. *Nat. Struct. Biol.* **1995**, *2*, 1095–1101. [[CrossRef](#)]
39. Royant, A.; Noirclerc-Savoie, M. Stabilizing role of glutamic acid 222 in the structure of Enhanced Green Fluorescent Protein. *J. Struct. Biol.* **2011**, *174*, 385–390. [[CrossRef](#)]
40. Guex, N.; Peitsch, M.C. SWISS-MODEL and the Swiss-Pdb Viewer: An environment for comparative protein modeling. *Electrophoresis* **1997**, *18*, 2714–2723. [[CrossRef](#)]
41. Ogino, H.; Wachi, M.; Ishii, A.; Iwai, N.; Nishida, T.; Yamada, S.; Nagai, K.; Sugai, M. FtsZ-dependent localization of GroEL protein at possible division sites. *Genes Cells* **2004**, *9*, 765–771. [[CrossRef](#)]
42. Sambrook, J.F.; Russell, D.W. *Molecular Cloning: A Laboratory Manual*, 3rd ed.; Cold Spring Harbor Laboratory Press: New York, NY, USA, 2001; ISBN 0-87969-577-3.
43. Kholod, N.; Mustelin, T. Novel vectors for co-expression of two proteins in *E. coli*. *Biotechniques* **2001**, *31*, 322–328. [[CrossRef](#)]
44. Gorokhovatsky, A.Y.; Rudenko, N.V.; Marchenkov, V.V.; Skosyrev, V.S.; Arzhanov, M.A.; Burkhardt, N.; Zakharov, M.V.; Semisotnov, G.V.; Vinokurov, L.M.; Alakhov, Y.B. Homogeneous assay for biotin based on *Aequorea victoria* bioluminescence resonance energy transfer system. *Anal. Biochem.* **2003**, *313*, 68–75. [[CrossRef](#)] [[PubMed](#)]
45. Figueiredo, L.; Klunker, D.; Ang, D.; Naylor, D.J.; Kerner, M.J.; Georgopoulos, C.; Hartl, F.U.; Hayer-Hartl, M. Functional characterization of an archaeal GroEL/GroES chaperonin system: Significance of substrate encapsulation. *J. Biol. Chem.* **2004**, *279*, 1090–1099. [[CrossRef](#)] [[PubMed](#)]
46. Ward, W.W. Biochemical and physical properties of green fluorescent protein. *Methods Biochem. Anal.* **2006**, *47*, 39–65. [[PubMed](#)]
47. Amemiya, Y.; Wakabayashi, K.; Hamanaka, T.; Wakabayashi, T.; Matsushita, T.; Hashizume, H. Design of small-angle X-ray diffractometer using synchrotron radiation at the photon factory. *Nucl. Instrum. Methods Phys. Res.* **1983**, *208*, 471–477. [[CrossRef](#)]

Disclaimer/Publisher’s Note: The statements, opinions and data contained in all publications are solely those of the individual author(s) and contributor(s) and not of MDPI and/or the editor(s). MDPI and/or the editor(s) disclaim responsibility for any injury to people or property resulting from any ideas, methods, instructions or products referred to in the content.